



Efficiency of electrochemical-synthesized alum nanoparticles in the removal of tannic acid as a precursor of carcinogenic trihalomethanes from drinking water: isotherm and kinetics study

Soudabeh Alizadeh Matboo^{a,b}, Kamal Hasani^{a,b}, Mina Moradi^{a,b}, Nazari Shahram^{b,*}, S. Ahmad Mokhtari^{b,*}

^aStudent Research Committee, School of Health, Ardabil University of Medical Sciences, Ardabil, Iran, emails: soudabehalizadeh@gmail.com (S.A. Matboo), kamalhasani.dudg@gmail.com (K. Hasani), moradimina38@yahoo.com (M. Moradi)

^bDepartment of Environmental Health Engineering, School of Public Health, Ardabil University of Medical Sciences, Ardabil, Iran, email: s.a.mokhtari@gmail.com (S. Ahmad Mokhtari)

Received 6 December 2020; Accepted 18 September 2021

ABSTRACT

In this experimental study, alum adsorbent was synthesized using an electrochemical process consisting of aluminum (anode) and iron (cathode) electrodes in a 1 L cylindrical reactor. The structure of the alum adsorbent was investigated using transmission electron microscopy, scanning electron microscopy, X-ray diffraction, and Brunauer–Emmett–Teller techniques. Adsorption process experiments were evaluated with four input parameters such as pH (4–9), alum nanoparticles dosage (0.01–0.05 g/L), initial concentration of tannic acid (10–80 mg/L), and contact time (5–50 min). The isotherm and adsorption kinetics were examined under optimal experimental conditions to evaluate the adsorption process. The results of the physicochemical analysis confirmed the accuracy of the alum structure. Under optimal conditions of the adsorption process, pH, adsorbent dose, initial concentration of tannic acid, and contact time were 6, 0.05 g/L, 20 mg/L, and 50 min; Under these conditions, the removal efficiency of tannic acid was obtained to be 93.9%. The results of the adsorption isotherm and kinetics studies showed that the adsorption process follows the Langmuir isotherm ($R^2 = 0.99$) while the process kinetics corresponds to the second-order kinetics model ($R^2 = 1$). The results showed that alum can be used as a high-availability and cost-effective adsorbent to remove tannic acid from aqueous solutions.

Keywords: Tannic acid; Alum; Electrochemical; Water-soluble; Adsorption isotherm; Adsorption kinetics

1. Introduction

Tannic acid is a water-soluble polyphenolic compound that is generated by the decomposition of organic matter in the environment and is frequently found in most surface and drinking waters. It has also been detected in the wastewater of cork and fiber factories, medicinal plants, paper, and leather industries [1]. Tannic acid is commonly found in

human diets including tea, beans, grapes, strawberries, etc., and is considered as a food additive and has antimicrobial activity and has antioxidant properties [2]. Although tannic acid has beneficial properties, it can cause serious and high-risk problems because the presence of this substance in drinking water may interfere with chlorine, which is a disinfectant in the water, and as a result, form carcinogenic products such as trihalomethanes [3]. These disinfection

* Corresponding authors.

by-products are approved or suspected of human carcinogenesis, which possibly causes cancers such as colorectal and bladder cancer [4]. In addition, tannic acid has received serious attention as an environmental pollutant due to its toxicity to aquatic organisms such as algae, phytoplankton, fish, and invertebrates [5]. Due to these cases, in order to protect the environment and public health, it is necessary to remove this contaminant from aqueous solutions. So far, many physical and chemical processes have been used to remove contaminants from aqueous solutions, including many types of nanostructures [6], nanofibers, and nanotubes [7]. Also, due to its simplicity and high efficiency, the adsorption method has been widely used in the removal of tannic acid from aqueous solutions. There are several adsorbents for the removal of tannic acid from aqueous solutions, the most common of which are activated carbon, resin, zirconium clay, chitosan, collagen fibers, and surfactant-modified clay [8]. These processes have problems such as high investment and operating costs and high sludge production, and even some of these technologies are not able to effectively remove tannic acid [9]; therefore, there is an urgent need to develop effective and efficient technologies to remove tannic acid from water. In recent years, advanced oxidation processes have attracted much attention for the removal of contaminants from aqueous solutions. One of these processes is the use of electrochemical techniques that have successfully helped the environment in developed countries [10]. The application of the electrochemical process in the water and wastewater industry is also very diverse. This technique has been used in various situations and industries to remove a wide range of pollutants [11,12]. This technique can be employed in water treatment, breaking fat and oil emulsions in water, removal of natural organic matter from water, defluoridation, removal of diazinon and sulfate compounds [13], removal of heavy metals [14], removal of phenolic compounds, treatment of baker's yeast production wastewater, treatment of mechanical polishing wastewater, as well as radioactive wastewater treatment. So far, various studies have been conducted on the use of electrochemical processes for the removal of pollutants. In his study, Matson designed an electrochemical mechanism to describe a device that had previously been proposed as an electronic coagulator. In another study, the removal of ammonia and nitrite from the aqueous solution in a batch reactor was investigated [15].

Electrochemical methods include electrical coagulation and electrical flotation. The electrocoagulation phase provides the destabilizing agents that cause the neutralization required to separate the contaminants. Electro-flotation also produces factors that promote interparticle bridging or coagulation, after which the formed complexes begin to precipitate. Thus, the removal of contaminants from the system can be achieved by removing sediments [16]. Electrocoagulation and flotation using sacrificial anodes have been extensively studied to remove suspended particles, organic compounds, dyes, metal ions and inorganic anions, and various combinations of water and wastewater [17]. The mechanism of stabilization of suspended particles of contaminants and breaking of emulsions in this process can be done by interparticle bridging, charge neutralization, ionic layer compression, and sweep coagulation.

The mechanism of action of the electrochemical process is described in reactions 1–3. In general, oxidation (reaction 1) and reduction (reaction 2) occur at the anode and cathode electrodes, respectively. Therefore, if an aluminum electrode is selected as the anode, these electrodes are decomposed according to (reaction 1), and aluminum hydroxides are produced (reaction 3) [18].



The aluminum hydroxides produced can be reused. If the water substrate used is pure water, the aluminum hydroxide produced does not require any purification and after drying at room temperature can be used directly to remove contaminants. Alum nanoparticles have features such as very low cost of synthesis, high availability, easy preparation in the laboratory, and having significant efficiency to remove contaminants [19]. On the other hand, given that the tannic acid in aqueous solutions has high importance and is a carcinogen, and no study has been done on the removal of tannic acid by the adsorption process using alum nanoparticles produced by the electrochemical process, this study was conducted to synthesize alum nanoparticles through the electrochemical process with electrodes of aluminum (anode) and iron (cathode) for removal of tannic acid as a precursor of trihalomethanes from aqueous solutions in different laboratory conditions and to achieve optimal removal conditions.

2. Materials and methods

2.1. Materials required

All chemicals and reagents were prepared in analytical with no more purification. The electrodes were made of aluminum and commercial iron plates. To adjust the pH of the solution, H_2SO_4 and NaOH (with 98% purity) were prepared from Merck Company, Germany. DC power device (model: Dazheng-PS-302D) was used as an electric power supply. The tannic acid powder was purchased commercially from Sigma Company and was used in the laboratory by preparing stock (1,000 mg/L) in different concentrations. The chemical structure of tannic acid is shown in Fig. 1 [20].

2.2. Construction of a reactor for the synthesis of alum nanoparticles

The electrochemical reactor consisted of an open Plexiglas chamber in which four electrodes (2 aluminum electrodes as anode and 2 iron electrodes as the cathode) were placed every other one in the row at 1 cm distance and were connected to a DC power source monopolar mode. A magnet was used to provide mixing inside the reactor during the process. The entire chamber was then placed on a magnetic stirrer at 200 rpm. The schematic of the electrochemical reactor is shown in Fig. 2.

2.3. Synthesis of alum nanoparticles

Prior to the synthesis of nanoparticles, the surface of the electrodes was sanded to remove impurities and then placed in HCl solution and then washed with distilled water for 1 min. Current density, synthesis time, distance between electrodes, and pH were considered to be 3.3 mA/cm², 5 h, 2 cm, and 7, respectively. After 5 h (reaction time), the contents of the suspension were allowed to settle for 30 min, and the supernatant was then removed using a pipette, and the nanoparticles were dried at ambient temperature for 72 h [21]. Transmission electron microscopy (TEM) was used to determine the size and morphology of alum nanoparticles. The morphology and crystallographic properties of the nanoparticles were also determined by scanning electron microscopy (SEM). The crystal structure of alum nanoparticles was determined by X-ray diffraction

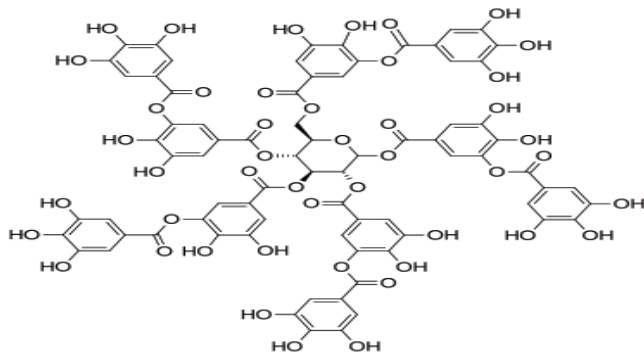


Fig. 1. Chemical structure of tannic acid.

(XRD). Brunauer–Emmett–Teller (BET) analysis was used to determine the specific surface area of nanoparticles.

2.4. Experimental procedure

This study was performed experimentally and on a laboratory scale. In order to perform the adsorption process, a 0.5 L cylindrical reactor was used. The sample volume at each stage of the experiment was 150 mL. Taking into account the two repetitions in the experiments, a total of 60 samples were tested in different conditions. Independent variables in this study included pH (4–9), alum nanoparticles dosage (0.01–0.05 g/L), initial concentration of tannic acid (10–80 mg/L), and contact time (5–50 min). Initially, the amount of tannic acid, pH value, and the alum nanoparticle dosage were selected 10 mg/L, 6 and 0.01–0.05 g/L, and at different times (5, 10, 20, 30, 50 min), the samples were taken to determine the optimal amount of alum nanoparticles. Then the amount of tannic acid in the range of 10–80 mg/L was tested to obtain the optimal concentration of tannic acid. After determining the optimal amount of alum nanoparticles and the concentration of tannic acid, the optimal pH value was determined using pH values of 4, 5, 6, 8, and 9. The maximum wavelength of tannic acid absorption was determined at 278 nm [22] by UV/VIS spectrophotometer (DR-5000). In order to measure the residual concentration of tannic acid, different samples were made with specific concentrations and their adsorption rate was read by spectrophotometer. The standard curve was then drawn based on the adsorption rate and specific concentrations. The outlet samples of the process were centrifuged at 30,000 rpm for 4 min, and after passing through a 0.45-micron filter, the residual concentration in the samples was measured.

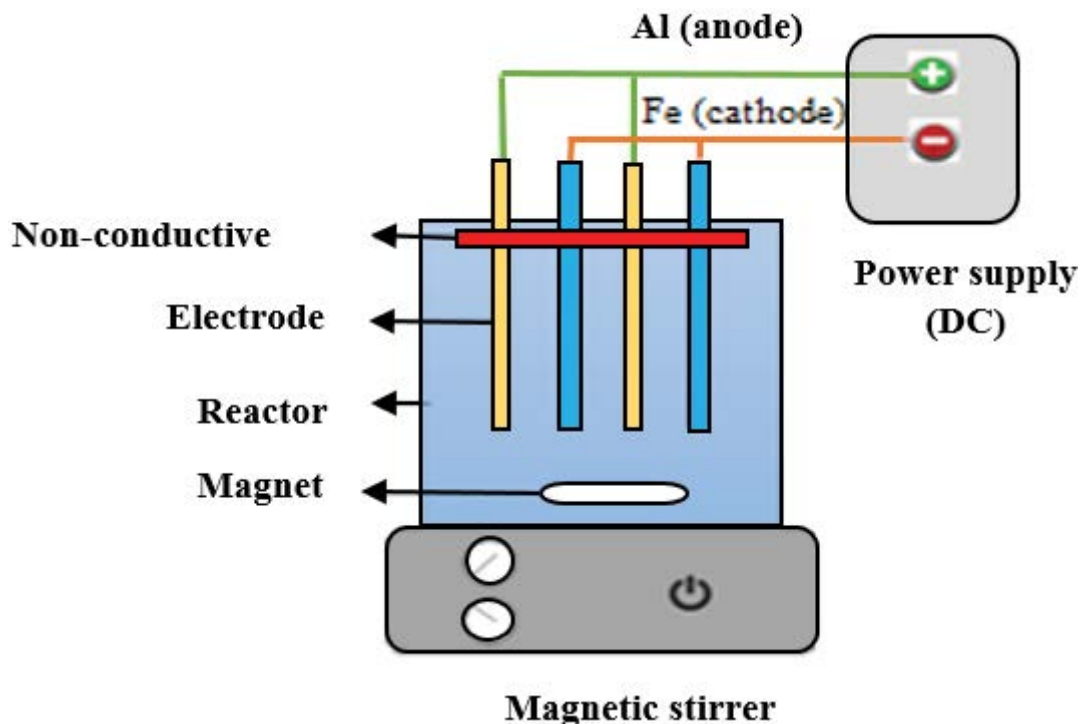


Fig. 2. Schematic of the electrochemical reactor and monopolar parallel electrodes.

Finally, by performing kinetic experiments, the adsorption capacity in equilibrium was calculated.

The adsorption rate of tannic acid on the adsorbent was denoted by q_e . The value of q_e was calculated using Eq. (4).

$$q_e = \frac{(C_i - C_f)V}{M} \quad (4)$$

In Eq. (4) C_i represents the initial concentration of the desired tannic acid solution (mg/L); C_f is the final concentration of the same solution (mg/L); V is the volume of the solution (L), and mass of the desired dry adsorbent mass (g).

Adsorption isotherms are used to predict and determine the adsorbent performance. In this study, Langmuir, Freundlich, and Temkin isotherms have been used; their equations and parameters are shown in Table 1. According to Table 1, q_e represents the equilibrium concentration of tannic acid in the solid phase (mg/g), C_e indicates the equilibrium concentration of tannic acid in the liquid phase (mg/L); q_m is the maximum adsorption capacity in mg/g, and K_L in the Langmuir isotherm, is energy related to chemical adsorption (L/mg). The basic characteristic of the Langmuir isotherm is expressed by a dimensionless constant called the equilibrium parameter, or R_L , which is defined in Eq. (5).

$$R_L = \frac{1}{1 + K_L C_0} \quad (5)$$

where, K_L is the Langmuir constant, and C_0 is the initial concentration of tannic acid (mg/L). R_L indicates the type of isotherm so that if $R_L = 0$ is irreversible; if $0 < R_L < 1$ is desirable; if $R_L = 1$ is linear, and if $R_L > 1$ is undesirable [23]. In Freundlich isotherm, K_F indicates the adsorption capacity at a unit concentration, and $1/n$ is the adsorption intensity. If $0 = 1/n$ is irreversible; if $0 < 1/n < 1$ is the desired state, and $1/n = 1$ is the undesirable state. In the Temkin isotherm, K_T also represents the Temkin constant.

To evaluate the adsorption mechanism, adsorption constants can be determined using first- and second-order kinetic equations [24]. The linear form of the first-order model in Eq. (6).

$$\log q_e - q_i = \log q_e - \frac{k_1}{2.303} t \quad (6)$$

where, q_e is the amount of tannic acid adsorbed at equilibrium (mg/g), q_i is the amount of tannic acid adsorbed at time t (mg/g), and k_1 is the equilibrium constant of the first-order kinetic rate (1/min).

The linear form of the second-order kinetic model for the adsorption of tannic acid by alum nanoparticles is as Eq. (7).

$$\frac{t}{q_i} = \frac{1}{k_2 q_e^2} + \frac{1}{q_e} t \quad (7)$$

where, q_e is the amount of tannic acid adsorbed at equilibrium (mg/g) and k_2 is the equilibrium rate constant of the second-order kinetic equation (g/mg min). The linear state between t/q_i and contact time (t) can be approximated by second-order kinetics.

The kinetic model of intraparticle diffusion based on the diffusion parameters in the adsorption processes is obtained using Eq. (8) [25].

$$q_i = k_p t^{1/2} + I \quad (8)$$

where, I represent the width of the origin and the constant k_p is the intracellular diffusion velocity (mg/g min^{1/2}).

3. Results

3.1. Determining the structural characteristics of the adsorbent

The surface properties of alum nanoparticles (corresponding diameter and morphology) by TEM are shown in Fig. 3a. Examination of the image shows that the particle size is almost spherical and has a smooth and uniform surface. The diameter of alum nanoparticles was approximately 25 nm. The crystallographic properties of alum nanoparticles by SEM analysis are shown in Fig. 3b. SEM analysis for alum nanoparticles showed a spherical structure with a size of approximately 100 nm. Fig. 3c identifies the crystal structures of alum nanoparticles by XRD. For alum nanoparticles, diffraction peaks with 2θ angle were observed at 18.45°, 20.46°, 27.79°, 37.47°, 40.54°, 44.79°, 52.53°, 58.41°, 63.95°, and 70.93°. The particle size of boehmite AlOOH using the Monshi et al. equation [26] was 90 nm. To describe the specific surface area of alum nanoparticles, the BET technique in Fig. 3d was used. The specific surface area of alum nanoparticles by BET analysis was obtained to be 109.79 m²/g. The pore volume and diameter of alum nanoparticles were 25.225 cm³/g and 2–50 nm, respectively.

3.2. Results of independent variables effect

3.2.1. Effect of pH

Fig. 4 shows the changes in the removal efficiency of tannic acid at different pH values. With increasing pH from

Table 1
Types of isotherms with equations and parameters used in this study

Isotherm	Equation	Linear form of the equation	Parameters
Langmuir	$q_e = (q_m K_L C_e) / (1 + K_L C_e)$	$C_e / q_e = (1 / K_L q_m) + (C_e / q_m)$	$q_m = (\text{slope})^{-1}$; $K_L = \text{slope} / \text{intercept}$
Freundlich	$q_e = K_F (C_e)^{1/n}$	$\ln q_e = \ln K_F + n^{-1} \ln C_e$	$K_F = \exp(\text{intercept})$; $n = (\text{slope})^{-1}$
Temkin	$q_e = q_m \ln(K_T C_e)$	$q_e = q_m \ln K_T + q_m \ln C_e$	$q_m = \text{slope}$; $K_T = \exp(\text{intercept} / \text{slope})$

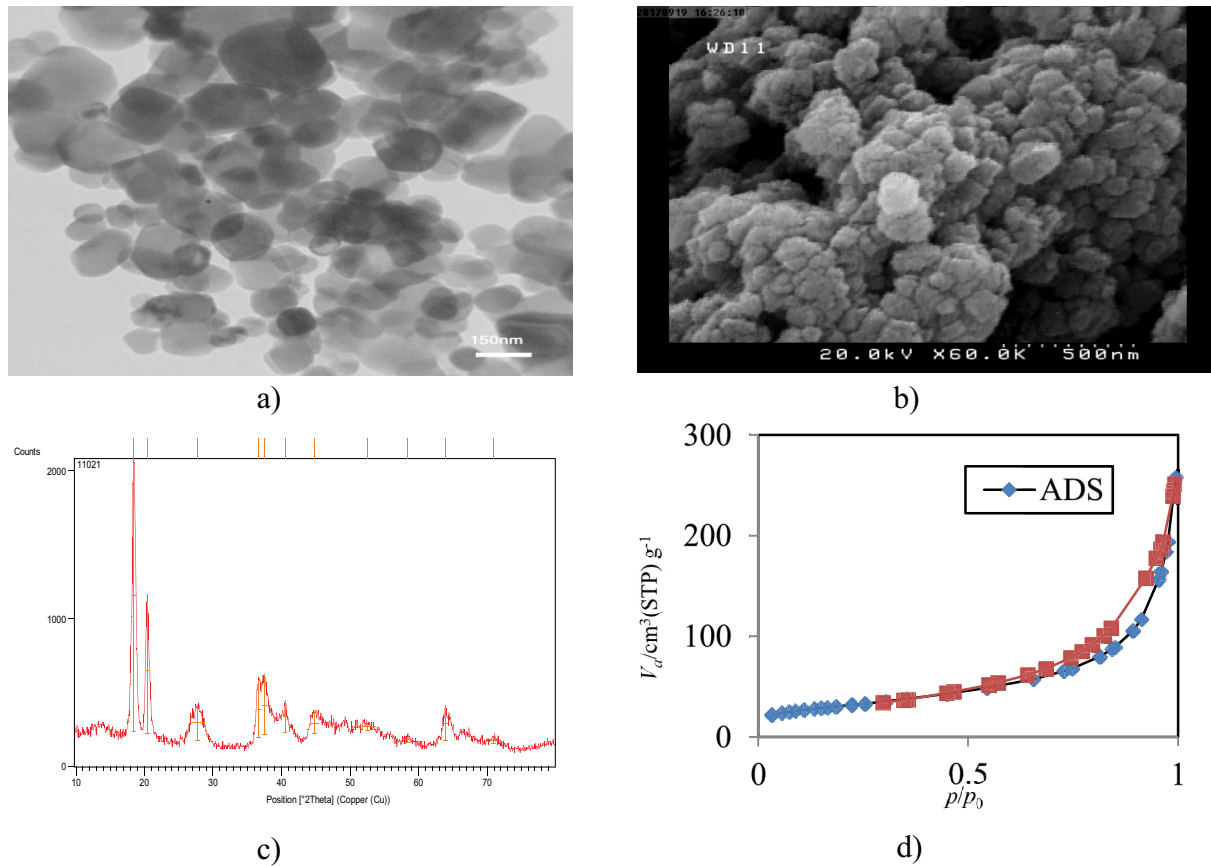


Fig. 3. (a) TEM, (b) SEM, (c) XRD, and (d) BET images related to the structural characteristics of alum nanoparticles.

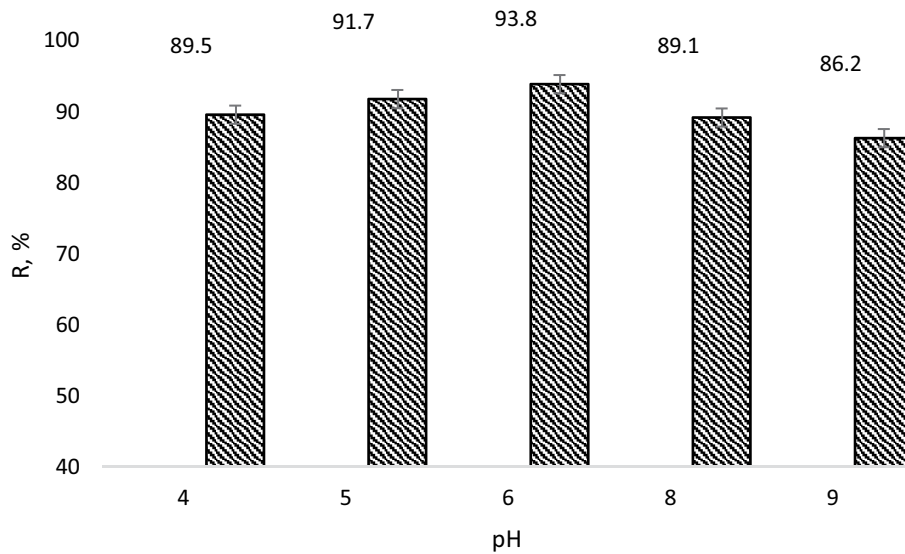


Fig. 4. Effect of pH on the tannic acid removal from aqueous solutions (alum nanoparticle dose: 0.05 g/L; initial tannic acid concentration: 20 mg/L; contact time: 50 min).

acidic to the state near neutral, the removal efficiency of tannic acid increased (pH = 6), while at the alkaline condition, the efficiency decreased again, and the efficiency of the process showed a decreasing trend. Under optimal conditions

of other variables (nanoparticle concentration of 0.05 g/L, initial tannic acid concentration of 20 mg/L, and contact time of 50 min) at pH of 4, the removal efficiency was 89.5%. With increasing pH to 6, efficiency to 93.8% increased, and

finally, at pH of 9, the removal efficiency decreased again and reached 86.2%. Therefore, the pH of 6 was selected as the optimal pH of the process to remove tannic acid.

3.2.2. Effect of initial concentration of alum nanoparticles

The different concentrations of alum nanoparticles were shown in Fig. 5. By increasing the dose of alum nanoparticles, the efficiency of the process for the removal of tannic acid has increased dramatically. With increasing the dose of nanoparticles from 0.01 to 0.05 g/L, the removal efficiency has increased from 83.4% to 93.9%. Based on this, the nanoparticle dose of 0.05 g/L was selected as the optimal dose.

3.2.3. Effect of initial concentration of tannic acid

Fig. 6 describes the effect of different concentrations of tannic acid on its removal efficiency in the adsorption process. With increasing the initial concentration of tannic

acid from 10 to 20 mg/L, the removal efficiency initially increased from 84.3% to 93.6%, but with changing the concentration of tannic acid from 20 to 80 mg/L, the removal efficiency decreased and reached 88.1% at a concentration of 80 mg/L. Therefore, a concentration of 20 mg/L of tannic acid was selected as the optimal concentration of the process.

3.3. Effect of contact time

Changes in the contact time of the adsorption process to remove tannic acid are shown in Fig. 7. As can be seen, at a contact time of 5 min, the removal efficiency of tannic acid is 85.3%. By increasing the contact time from 5 to 10 min, the removal efficiency increased to 88.1%. Then, with increasing the contact time, the removal efficiency of tannic acid gradually increased, and finally, at a contact time of 50 min, the removal efficiency reached 93.9%. Therefore, the optimal time for the process equilibrium was considered to be 50 min.

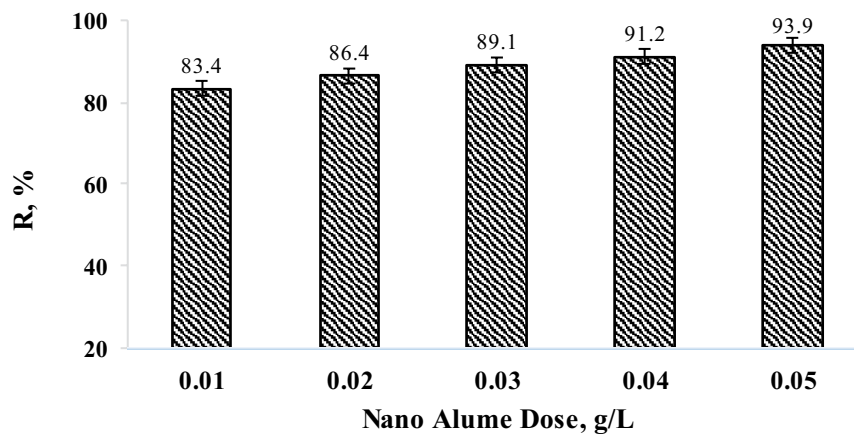


Fig. 5. Effect of initial concentration of alum nanoparticles on the removal of tannic acid from aqueous solutions (initial tannic acid concentration: 20 mg/L; pH: 6; contact time: 50 min).

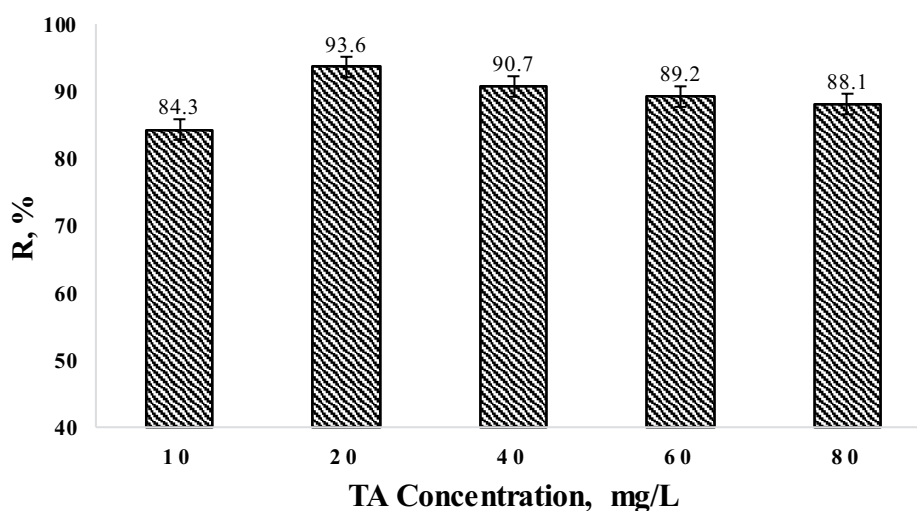


Fig. 6. Effect of initial concentration of tannic acid on its removal from aqueous solutions (alum nanoparticle dose: 0.5 g/L; pH: 6; contact time: 50 min).

3.4. Tannic acid removal efficiency under optimal conditions

After performing experiments related to parameters including pH, alum nanoparticles dosage, initial concentration of tannic acid, and contact time in different conditions and by repeating the experiments twice, the optimal conditions of the independent variables of the present study were obtained. Thus, pH of 6, alum nanoparticles dosage of 0.05 g/L, the initial tannic acid concentration of 20 mg/L, and contact time of 50 min were determined as the optimal state. Under the above optimal conditions, the removal efficiency of tannic acid by alum adsorbent synthesized by electrochemical process reached 93.9%.

3.5. Investigation of isotherm and adsorption kinetics

Adsorption isotherms are very important from a theoretical and practical point of view in processes. For this purpose, Langmuir, Freundlich, and Temkin models were studied to evaluate the interaction between tannic acid and adsorbent and pollutant adsorption capacity. The results of isotherm parameters of three types of Langmuir, Freundlich, and Temkin isotherms in adsorption of tannic acid by alum nanoparticles were shown in Table 2 and Fig. 8a–c. By comparing the isotherm parameters in three different models, it was observed that the value of correlation coefficient (R^2) in the Langmuir model is approximately close

to 1 ($R^2 = 0.99$), so it can be said that the adsorption process follows the Langmuir isotherm.

The results of kinetic constants of adsorption of tannic acid by alum nanoparticles were presented in Table 3 and Fig. 9a–c. In this study, the first-order and second-order adsorption kinetics and intraparticle diffusion under optimal conditions were investigated. The results showed that the correlation coefficient (R^2) of the second-order kinetics in the adsorption of tannic acid by alum nanoparticles was 1. Accordingly, according to the obtained constant coefficients and correlations, it can be said that the process follows the second-order kinetic model.

4. Discussion

TEM images are used for a more detailed study of the physical structure and surface morphology of nanoparticles. In the present study, the TEM image showed the particle size as spherical and uniform. In the study of Mittal et al. [27], the spherical structure of Fe_3O_4 nanoparticles used for the removal of green malachite dye was analyzed by TEM images. In another study by Sun et al. [28], the spherical shape of poly iron, aluminum silicate, and sulfate nanoparticles from ash analyzed by TEM was approximately 25–30 nm. The study of the physical structure and morphology of the surface of alum nanoparticles was analyzed using SEM images. SEM analysis for nanoparticles showed

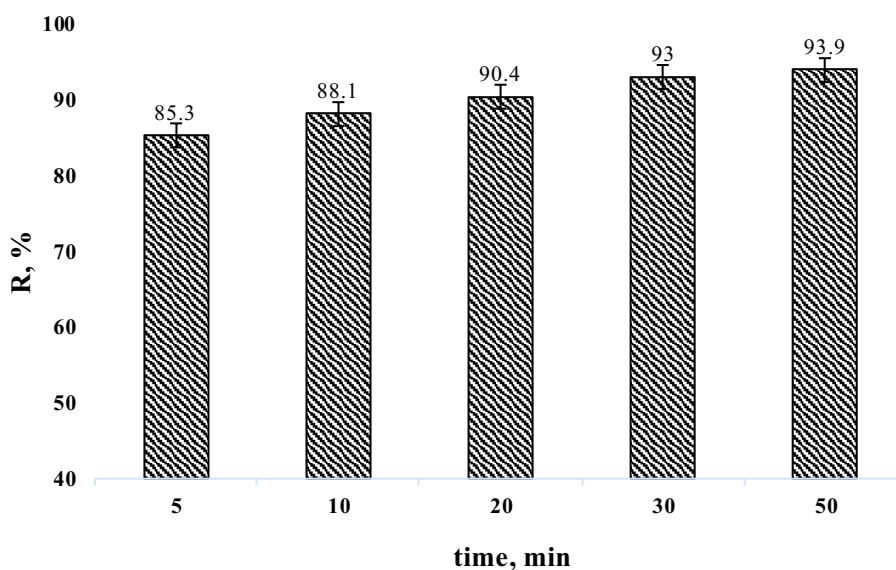


Fig. 7. Effect of contact time on the removal of tannic acid from aqueous solutions (nanoparticle concentration: 0.05 g/L; initial tannic acid concentration: 20 mg/L; pH: 6).

Table 2

Results of isotherms of tannic acid adsorption by alum nanoparticles (adsorbent concentration: 0.05 g/L; initial concentration of tannic acid: 20 mg/L; pH: 6)

Isotherm	Langmuir isotherm				Freundlich isotherm			Temkin isotherm			
	q_e (EX)	q_m (mg/g)	K_L (L/mg)	R_L	R^2	K_F (mg/g)	N	R^2	q_m (mg/g)	K_T (L/mg)	R^2
	375.9	375.9	0.0702	0.064	0.99	352.02	4.81	0.98	90.04	90.35	0.95

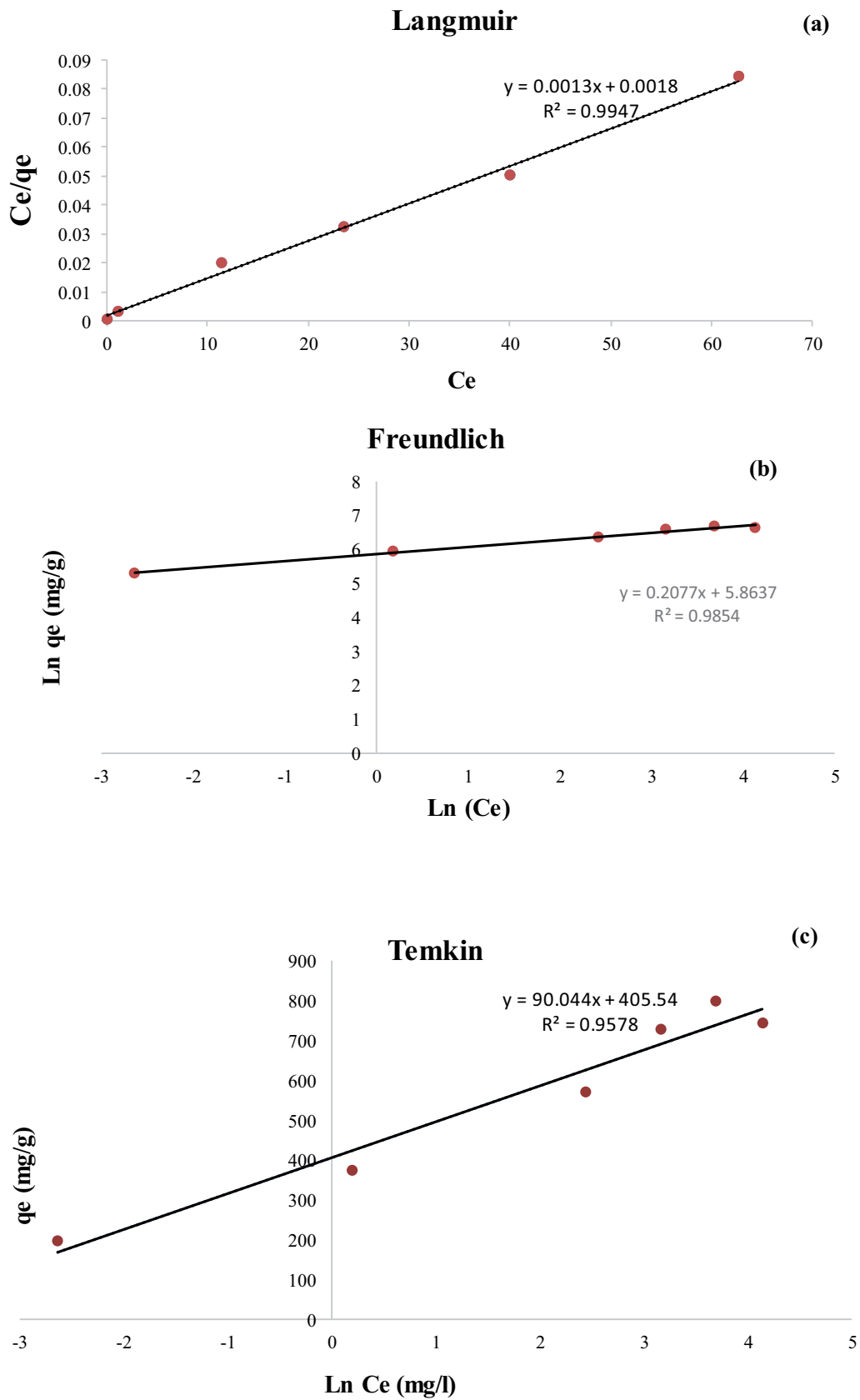


Fig. 8. The linear form of Langmuir (a), Freundlich (b) and Temkin (c) isotherms equations for tannic acid on the alum nanoparticle surface.

Table 3

Results of kinetic parameters of tannic acid adsorption by alum nanoparticles (adsorbent concentration: 0.05 g/L; initial tannic acid concentration: 20 mg/L; pH: 6)

Kinetic	First-order kinetics			Second-order kinetics			Intraparticle penetration			
	q_e (EX)	$(q_e)_{Cal}$	k_1	R^2	$(q_e)_{Cal}$	k_2	R^2	k_p	I	R^2
	375.9	9.07	0.063	0.78	370.3	0.018	1	1.71	364.5	0.73

an almost spherical structure with a size of approximately 100 nm. In the study of Liuzhang et al. [29], SEM analysis showed approximately similar results for morphology and crystallographic properties of Al₂O₃ nanoparticles [29]. The crystal structure of alum nanoparticles was determined by the XRD method. Diffraction peaks with a 2 θ angle were observed in the results of this study, and the particle size was obtained to be 90 nm, which was in line with the Monshi et al. study [26]. The results of BET analysis showed that the surface area was 109.79 m²/g, and the pore volume and pore diameter of alum were 25.225 cm³/g and 3.50 nm, respectively. The study conducted by Wang et al. [30] on the use of alum sludge for the production of aluminum hydroxide in the chemical coagulation process showed that following changes in temperature, surface, and volume of particles increased from 5.8 to 95.6 m²/g and from 0.008 to 0.414 cm³/g, respectively. Yang et al. [31] conducted another study based on BET analysis using alum sludge pore structure and reported that the specific surface area of alum sludge was 49.03, which was significantly related to the present study.

In adsorption processes, the pH factor plays an important role in removing contaminants from aqueous solutions and is one of the important components of the water and wastewater quality parameter that can affect the adsorption capacity by changing the adsorbent surface. In Fig. 4, with increasing the pH from the acidic to the state near to neutral (pH = 6), the process efficiency has increased, but at alkaline conditions, the removal efficiency has gradually decreased. On the other hand, the optimal pH value of alum is in the range of 5–7 because at this pH, aluminum hydroxide (Al(OH)₃) flocs have the least solubility [32].

In a study, Yang et al. treated the river water by coagulation process using aluminum persulfate (alum) and poly-aluminum chloride, and found the highest process efficiency at pH = 6 as the optimal state, the results of which were consistent with the present study [33]. At low pH values, the positive charge density at the adsorbent surface increases, and the electrostatic attraction force significantly increases between the positive surface charge of the adsorbent and the contaminant molecules, which leads to improving the distribution and dispersion of the contaminant [34].

In a study conducted for the adsorption of tannic acid using amine group activated silica adsorbent, it was noted that the maximum adsorption capacity of tannic acid is 512.2 mg/g and its adsorption is strongly dependent on pH and ionic strength and electrostatic reactions play a crucial role in the adsorption of tannic acid [35]. Adsorbent concentration is an effective and important factor in adsorption processes because the amount of tannic acid removed and the amount of adsorbent consumed and, as a result, the cost

of the operation is affected [36]. In the present study, the efficiency of the process was slightly increased by increasing the adsorbent dose. The high efficiency of the process and the increase in the adsorption of tannic acid are due to the increase in the number of active sites, the increase in the adsorbent surface, and the presence of a strong driving force that occurs due to an increase in the initial dose of the adsorbent [37]. The results of the study by Sun et al. [38] revealed that by increasing the dose of polyaniline adsorbent, tannic acid removal efficiency was increased; this is almost consistent with the present study. One of the most important factors, which should be considered in the adsorption of contaminants, is the effect of the initial concentration of the adsorbate. In this study, with increasing the initial concentration of tannic acid from 10 to 20 mg/L, the efficiency initially increased, but with increasing the concentration of contaminants, the removal efficiency gradually decreased, and the removal efficiency was higher at low concentrations. On the other hand, considering that for a certain amount of adsorbent, its active surface is constant, so with increasing the initial concentration of contaminants, process efficiency decreases due to the shortage of active sites at the adsorbent surface. Adsorbents have also limited adsorption sites that, as the initial concentration of the contaminant increased, their capacity is saturated more rapidly and the removal efficiency decreased [39,40]. The results of the study conducted by Sarıcı-Özdemir and Önal [8] showed that with increasing the initial concentration of tannic acid, the adsorption efficiency onto activated carbon decreases, which was in line with the results of the present study. One of the important factors in the adsorption process is the effect of contact time, which is directly related to the adsorption capacity and removal efficiency of tannic acid. In the present study, with a gradual increase in contact time from 5 to 50 min, the removal efficiency of tannic acid increased and the highest removal efficiency was obtained at high contact times. In general, the adsorption capacity increases with time and at a certain time reaches a constant value and no molecule of tannic acid is removed from the solution. Adsorption of tannic acid rapidly occurred in the early stages of treatment time and slowed down near equilibrium. It is clear that in the early stages, a large number of empty surface sites are available for adsorption, and over time, it remains difficult to occupy the remaining empty sites because a repulsion between the adsorbed tannic acid on the solid surface and the molecules in the solution phase occurs [41]. Various studies have shown the positive effect of contact time for high efficiency of the adsorption process for optimal removal of the contaminant, the results of which were consistent with the present study [42,43].

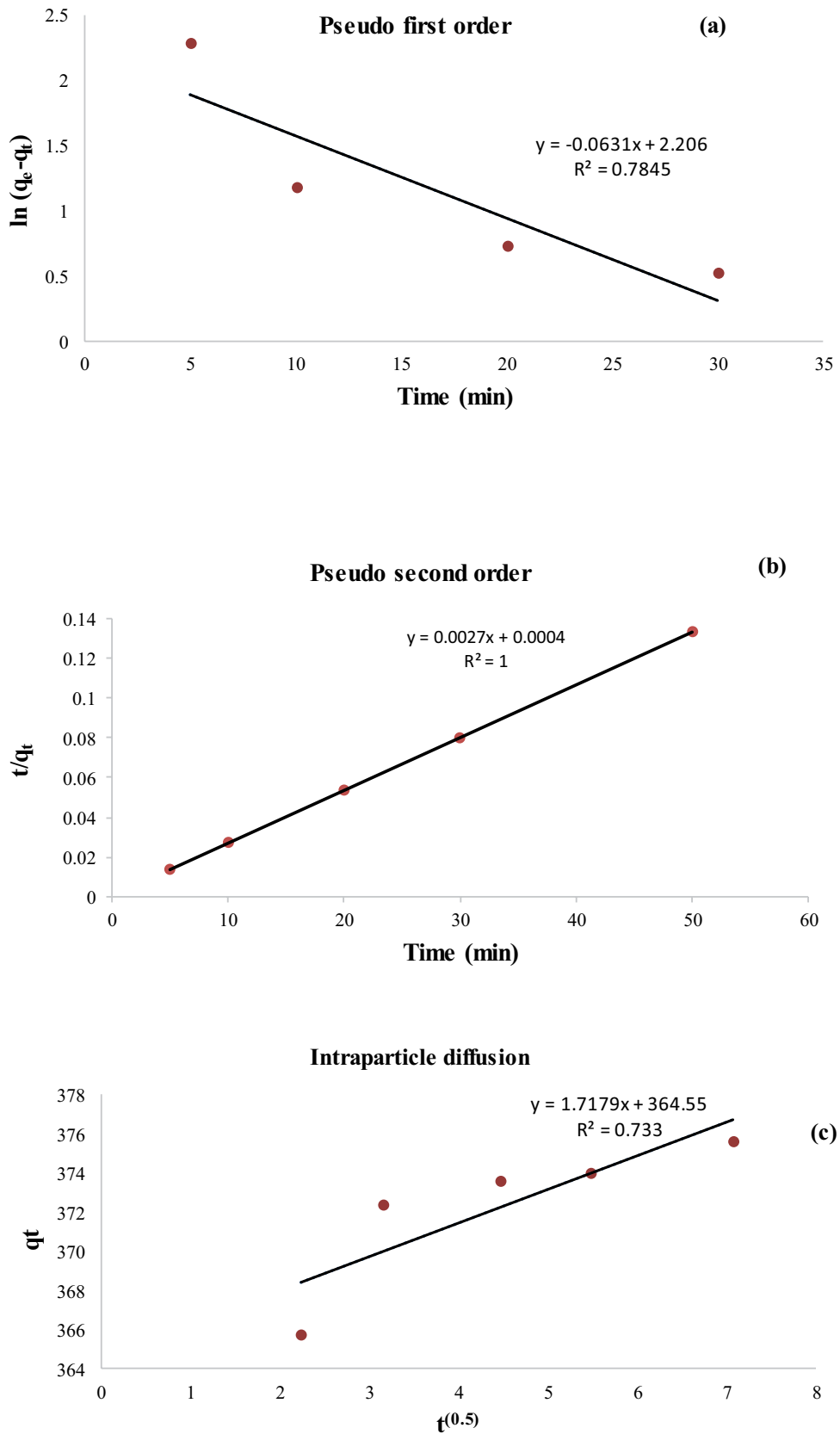


Fig. 9. Pseudo-first-order (a), pseudo-second-order (b) and intraparticle diffusion (c) kinetics models for tannic acid on alum nanoparticle surface.

The findings of Zhou and Haynes [44] study showed that alum adsorbent has a significant efficiency in removing Pb(II) and Cr(III and VI) metals from aqueous solutions and this adsorbent effectively increases the removal efficiency of contaminants. The study of Poorsadeghi et al. [45] showed that the removal efficiency of arsenic from water using synthesized alum nanoparticles reached 92%. These findings were largely consistent with the present study and show that alum nanoparticles are effective in removing pollutants from various aquatic environments.

Adsorption isotherms designate how contaminants react with adsorbents and play a key role in optimizing adsorption consumption. In this study, three types of Langmuir, Freundlich, and Temkin isotherms have been investigated. Process isotherm studies showed that the process follows the Langmuir isotherm model. The Langmuir isotherm is one of the simplest types of isotherms that can provide information on the adsorption capabilities of the adsorbent and can express the equilibrium behavior of the adsorption process. This isotherm shows the relationship between the contaminant range in the solid phase (adsorbent) and the liquid phase (solution) [46]. The Langmuir isotherm assumes that the adsorbent surface is perfectly uniform and that each active site of the adsorbent can absorb a maximum of one adsorbate molecule, so the adsorbed layers will be one molecule thick (single layer). In addition, it is assumed that all adsorption sites have the same affinity for adsorbate molecules and that there is no interaction between adsorbate molecules. In Freundlich isotherm, the adsorbent has a non-uniform surface that is composed of different levels of adsorption sites. The Temkin isotherm explains that the adsorption heat of all molecules on the adsorbent surface decreases linearly with the amount of surface coverage due to the adsorption-adsorption interactions; therefore, the adsorption potential of the adsorbent for adsorbates can be evaluated with the Temkin isotherm in which the decrease in adsorption heat is linear [47].

The adsorption capacity of alum nanoparticle for tannic acid from isotherm of Langmuir was compared with that reported by other studies using other adsorbents. According to Table 4, the adsorption of alum for tannic acid is very effective compared to other adsorbents. Therefore, the alum nanoparticle adsorbent has a super adsorption ability of tannic acid.

In order to provide information about the factors affecting the reaction rate, kinetic evaluation is necessary. Kinetic models that are widely used in sources for adsorption

processes include first-order, second-order kinetics, and intraparticle diffusion. These kinetic models are used to determine the control mechanism of adsorption processes, such as surface adsorption, chemical reaction, or diffusion mechanisms [51]. The results of the present study showed that the adsorption process follows the second-order kinetic model. The second-order kinetics is an interesting and useful model because various studies have shown that the kinetics of most adsorption systems in different concentrations of pollutants and different amounts of adsorbent are well compatible with this system [52,53].

5. Conclusion

In this study, the nature and structure of alum adsorbent were confirmed using TEM, SEM, XRD, and BET analyses. After performing the experiments, the optimal conditions for the removal of tannic acid with alum nanoparticles were obtained (pH = 6, alum nanoparticles dosage = 0.05 g/L, initial tannic acid concentration = 20 mg/L, and contact time = 50 min) and under these conditions, the removal efficiency reached 93.9%. Based on the findings of the isotherm and kinetics study, the adsorption process follows the Langmuir isotherm ($R^2 = 0.99$) and the second-order kinetics ($R^2 = 1$). The results showed that through employment of alum nanoparticles, the highest tannic acid removal efficiency is obtained by the adsorption process, and alum can be used as a high-availability and cost-effective adsorbent to remove tannic acid from aqueous solutions.

Acknowledgments

This research is the result of a research project approved by the Student Research Committee of Ardabil University of Medical Sciences. We hereby express our gratitude and appreciation to the esteemed Research deputy of the University for the Financial Support of the project and the esteemed officials of the Laboratory of Environmental Chemistry and Microbiology of the Faculty of Health.

References

- [1] W. Li, X. Li, K. Zeng, Aerobic biodegradation kinetics of tannic acid in activated sludge system, *Biochem. Eng. J.*, 14 (2009) 142–148.
- [2] R. Kumar, M. Barakat, E.M. Soliman, Removal of tannic acid from aqueous solution by magnetic carbohydrate natural polymer, *J. Ind. Eng. Chem.*, 20 (2014) 2992–2997.
- [3] J. Wang, A. Li, L. Xu, Y. Zhou, Adsorption of tannic and gallic acids on a new polymeric adsorbent and the effect of Cu(II) on their removal, *J. Hazard. Mater.*, 169 (2009) 794–800.
- [4] M. Gholami, S. Nazari, M. Farzadkia, G. Majidi, S.A. Matboo, Assessment of nanopolyamidoamine-G7 dendrimer antibacterial effect in aqueous solution, *Tehran Univ. Med. J.*, 74 (2016) 159–167.
- [5] E. De Nicola, S. Meriç, M. Gallo, M. Iaccarino, C. Della Rocca, G. Lofrano, T. Russo, G. Pagano, Vegetable and synthetic tannins induce hormesis/toxicity in sea urchin early development and in algal growth, *Environ. Pollut.*, 146 (2007) 46–54.
- [6] M. Gholami, S. Nazari, M. Farzadkia, S.M. Mohseni, S.A. Matboo, F.A. Dourbash, M. Hasannejad, Nano polyamidoamine-G7 dendrimer synthesis and assessment of the antibacterial effect in vitro, *Tehran Univ. Med. J.*, 74 (2016) 25–35.
- [7] M. Adabi, R. Saber, R. Faridi-Majidi, F. Faridbod, Performance of electrodes synthesized with polyacrylonitrile-based carbon

Table 4
Isotherm models parameters and comparison of adsorption capacities of tannic acid of different adsorbents

Adsorbent	Q_{max} (mg/g)	References
Clay	153	[48]
Chitosan-montmorillonite	240	[49]
$Fe_3O_4@SiO_2-NH_2$	140.85	[22]
magMCM-41- NH_2	225.3	[35]
Polyaniline	225	[38]
Biochar	67.41	[50]

- nanofibers for application in electrochemical sensors and biosensors, *Mater. Sci. Eng., C*, 48 (2015) 673–678.
- [8] Ç. Sarıci-Özdemir, Y. Önal, Equilibrium, kinetic and thermodynamic adsorptions of the environmental pollutant tannic acid onto activated carbon, *Desalination*, 251 (2010) 146–152.
- [9] A.R. Rahmani, H.R. Ghafari, M.T. Samadi, M. Zarabi, Synthesis of zero valent iron nanoparticles (nZVI) and its efficiency in arsenic removal from aqueous solutions, *Water Wastewater*, 1 (2011) 35–41.
- [10] P.K. Holt, G.W. Barton, M. Wark, C.A. Mitchell, A quantitative comparison between chemical dosing and electrocoagulation, *Colloids Surf., A*, 211 (2002) 233–248.
- [11] L.J.J. Janssen, L. Koene, The role of electrochemistry and electrochemical technology in environmental protection, *Chem. Eng. J.*, 85 (2002) 137–146.
- [12] M. Pirsaeheb, E. Azizi, A. Almasi, M. Soltanian, T. Khosravi, M. Ghayebzadeh, K. Sharafi, Evaluating the efficiency of electrochemical process in removing COD and $\text{NH}_4\text{-N}$ from landfill leachate, *Desal. Water Treat.*, 57 (2016) 6644–6651.
- [13] M. Heidari, M. Vosoughi, H. Sadeghi, A. Dargahi, S.A. Mokhtari, Degradation of diazinon from aqueous solutions by electro-Fenton process: effect of operating parameters, intermediate identification, degradation pathway, and optimization using response surface methodology (RSM), *Sep. Sci. Technol.*, 56 (2020) 2287–2299.
- [14] Keerthi, V. Vinduja, N. Balasubramanian, Removal of heavy metals by hybrid electrocoagulation and microfiltration processes, *Environ. Technol.*, 34 (2013) 2897–2902.
- [15] M. Saleem, M. Chakrabarti, D.B. Hasan, Electrochemical removal of nitrite in simulated aquaculture wastewater, *Afr. J. Biotechnol.*, 10 (2011) 16566–16576.
- [16] W.W. Eckenfelder, L.K. Cecil, Applications of New Concepts of Physical–Chemical Wastewater Treatment, Vol. 1, Vanderbilt University, Nashville, Tennessee, Elsevier, Amsterdam, September 18–22, 1972.
- [17] N. Balasubramanian, T. Kojima, C. Srinivasakannan, Arsenic removal through electrocoagulation: kinetic and statistical modelling, *Chem. Eng. J.*, 155 (2009) 76–82.
- [18] N.A. Fayad, T. Yehya, F. Audonnet, Ch. Vial, Preliminary purification of volatile fatty acids in a digestate from acidogenic fermentation by electrocoagulation, *Sep. Purif. Technol.*, 184 (2017) 220–230.
- [19] D.J. Naghan, M.D. Motevalli, N. Mirzaei, A. Javid, H.R. Ghaffari, M. Ahmadpour, M. Moradi, K. Sharafi, Efficiency comparison of alum and ferric chloride coagulants in removal of dye and organic material from industrial wastewater - a case study, *Bulg. Chem. Commun.*, 47 (2015) 206–210.
- [20] Y. Zhou, X.-H. Xing, Z. Liu, L. Cui, A. Yu, Q. Feng, H. Yang, Enhanced coagulation of ferric chloride aided by tannic acid for phosphorus removal from wastewater, *Chemosphere*, 72 (2008) 290–298.
- [21] B. Hayati, S. Nazari, S.A. Matboo, H. Pasalari, M. Arzanlou, E. Asgari, S.M. Mohseni, Improvement on electrochemical inactivation of *Escherichia coli* and *Clostridium perfringens* by assisted alum nanocrystallites approach: parametric and cost evaluation, *Desal. Water Treat.*, 207 (2020) 361–372.
- [22] J. Wang, C. Zheng, S. Ding, H. Ma, Y. Ji, Behaviors and mechanisms of tannic acid adsorption on an amino-functionalized magnetic nano-adsorbent, *Desalination*, 273 (2011) 285–291.
- [23] T. Bohli, A. Ouederni, N. Fiol, I. Villaescusa, Evaluation of an activated carbon from olive stones used as an adsorbent for heavy metal removal from aqueous phases, *C.R. Chim.*, 18 (2015) 88–99.
- [24] E. Antunes, M.V. Jacob, G. Brodie, P.A. Schneider, Silver removal from aqueous solution by biochar produced from biosolids via microwave pyrolysis, *J. Environ. Manage.*, 203 (2017) 264–272.
- [25] P. Thilagavathy, T. Santhi, Kinetics, isotherms and equilibrium study of Co(II) adsorption from single and binary aqueous solutions by *Acacia nilotica* leaf carbon, *Chin. J. Chem. Eng.*, 22 (2014) 1193–1198.
- [26] A. Monshi, M.R. Foroughi, M.R. Monshi, Modified Scherrer equation to estimate more accurately nano-crystallite size using XRD, *World J. Nano Sci. Eng.*, 2 (2012) 154–160.
- [27] H. Mittal, V. Parashar, S.B. Mishra, A.K. Mishra, Fe_3O_4 MNPs and gum xanthan based hydrogels nanocomposites for the efficient capture of malachite green from aqueous solution, *Chem. Eng. J.*, 255 (2014) 471–482.
- [28] T. Sun, C.-h. Sun, G.-l. Zhu, X.-j. Miao, C.-c. Wu, S.-b. Lv, W.-j. Li, Preparation and coagulation performance of poly-ferric-aluminum-silicate-sulfate from fly ash, *Desalination*, 268 (2011) 270–275.
- [29] O. Liuzhang, L. Chengping, S. Xiandong, Z. Meiqin, Z. Min, Fabrication and microstructure of in situ Al_2O_3 decomposed from $\text{Al}_2(\text{SO}_4)_3$ -reinforced aluminum matrix composites, *Mater. Lett.*, 57 (2003) 1712–1715.
- [30] L.Y. Wang, D.S. Tong, L.Z. Zhao, F.G. Liu, N. An, W.H. Yu, C.H. Zhou, Utilization of alum sludge for producing aluminum hydroxide and layered double hydroxide, *Ceram. Int.*, 40 (2014) 15503–15514.
- [31] Y. Yang, Y. Zhao, P. Kearney, Influence of ageing on the structure and phosphate adsorption capacity of dewatered alum sludge, *Chem. Eng. J.*, 145 (2008) 276–284.
- [32] Z.L. Yang, B.Y. Gao, Q.Y. Yue, Y. Wang, Effect of pH on the coagulation performance of Al-based coagulants and residual aluminum speciation during the treatment of humic acid-kaolin synthetic water, *J. Hazard. Mater.*, 178 (2010) 596–603.
- [33] Z. Yang, B. Gao, Q. Yue, Coagulation performance and residual aluminum speciation of $\text{Al}_2(\text{SO}_4)_3$ and polyaluminum chloride (PAC) in Yellow River water treatment, *Chem. Eng. J.*, 165 (2010) 122–132.
- [34] A. Safa Özcan, A. Özcan, Adsorption of acid dyes from aqueous solutions onto acid-activated bentonite, *J. Colloid Interface Sci.*, 276 (2004) 39–46.
- [35] J. Wang, S. Zheng, J. Liu, Z. Xu, Tannic acid adsorption on amino-functionalized magnetic mesoporous silica, *Chem. Eng. J.*, 165 (2010) 10–16.
- [36] M.M. Salim, N.A.N.N. Malek, Characterization and antibacterial activity of silver exchanged regenerated NaY zeolite from surfactant-modified NaY zeolite, *Mater. Sci. Eng., C*, 59 (2016) 70–77.
- [37] Y. Deng, L. Wang, X. Hu, B. Liu, Z. Wei, S. Yang, C. Sun, Highly efficient removal of tannic acid from aqueous solution by chitosan-coated attapulgite, *Chem. Eng. J.*, 181 (2012) 300–306.
- [38] C. Sun, B. Xiong, Y. Pan, H. Cui, Adsorption removal of tannic acid from aqueous solution by polyaniline: analysis of operating parameters and mechanism, *J. Colloid Interface Sci.*, 487 (2017) 175–181.
- [39] Y. Ge, Z. Li, Y. Kong, Q. Song, K. Wang, Heavy metal ions retention by bi-functionalized lignin: synthesis, applications, and adsorption mechanisms, *J. Ind. Eng. Chem.*, 20 (2014) 4429–4436.
- [40] J. Antony, Design of Experiments for Engineers and Scientists, Elsevier, Amsterdam, 2014.
- [41] P. Wang, M. Du, H. Zhu, S. Bao, T. Yang, M. Zou, Structure regulation of silica nanotubes and their adsorption behaviors for heavy metal ions: pH effect, kinetics, isotherms and mechanism, *J. Hazard. Mater.*, 286 (2015) 533–544.
- [42] S.S. Tripathy, J.-L. Bersillon, K. Gopal, Removal of fluoride from drinking water by adsorption onto alum-impregnated activated alumina, *Sep. Purif. Technol.*, 50 (2006) 310–317.
- [43] N. Mohammadi, H. Khani, V.K. Gupta, E. Amereh, S. Agarwal, Adsorption process of methyl orange dye onto mesoporous carbon material—kinetic and thermodynamic studies, *J. Colloid Interface Sci.*, 362 (2011) 457–462.
- [44] Y.-F. Zhou, R.J. Haynes, Removal of Pb(II), Cr(III) and Cr(VI) from aqueous solutions using alum-derived water treatment sludge, *Water Air Soil Pollut.*, 215 (2011) 631–643.
- [45] S. Poorsadeghi, M. Kassaee, H. Fakhri, M. Mirabedini, Removal of arsenic from water using aluminum nanoparticles synthesized through arc discharge method, *Iran. J. Chem. Chem. Eng.*, 36 (2017) 91–99.
- [46] I.H. Chowdhury, A.H. Chowdhury, P. Bose, S. Mandal, M.K. Naskar, Effect of anion type on the synthesis of mesoporous nanostructured MgO, and its excellent adsorption capacity for the removal of toxic heavy metal ions from water, *RSC Adv.*, 6 (2016) 6038–6047.

- [47] M. Tony, Zeolite-based adsorbent from alum sludge residue for textile wastewater treatment, *Int. J. Environ. Sci. Technol.*, 17 (2020) 2485–2498.
- [48] M.-Y. Chang, R.-S. Juang, Adsorption of tannic acid, humic acid, and dyes from water using the composite of chitosan and activated clay, *J. Colloid Interface Sci.*, 278 (2004) 18–25.
- [49] J.-H. An, S. Dultz, Adsorption of tannic acid on chitosan-montmorillonite as a function of pH and surface charge properties, *Appl. Clay Sci.*, 36 (2007) 256–264.
- [50] A.A. Lawal, M.A. Hassan, M.A.A. Farid, T.A.T. Yasim-Anuar, M.H. Samsudin, M.Z.M. Yusoff, M.R. Zakaria, M.N. Mokhtar, Y. Shirai, Adsorption mechanism and effectiveness of phenol and tannic acid removal by biochar produced from oil palm frond using steam pyrolysis, *Environ. Pollut.*, 269 (2021) 116–197.
- [51] C.-B. Cai, L. Xu, W. Zhong, Y.-Y. Tao, B. Wang, H.-W. Yang, M.-Q. Wen, Studying a gas–solid multi-component adsorption process with near-infrared process analytical technique: experimental setup, chemometrics, adsorption kinetics and mechanism, *Chemom. Intell. Lab. Syst.*, 144 (2015) 80–86.
- [52] K. Ahamad, R. Singh, I. Baruah, H. Choudhury, M. Sharma, Equilibrium and kinetics modeling of fluoride adsorption onto activated alumina, alum and brick powder, *Groundwater Sustainable Dev.*, 7 (2018) 452–458.
- [53] Y. Xiao, J. Azaiez, J.M. Hill, Erroneous application of pseudo-second-order adsorption kinetics model: ignored assumptions and spurious correlations, *Ind. Eng. Chem. Res.*, 57 (2018) 2705–2709.